

Photo-rechargeability of TiO₂/LiMn₂O₄ Bi-layer Film Electrodes Prepared by Pulsed Laser Deposition

H. Usui, O. Miyamoto, T. Nomiya, Y. Horie and T. Miyazaki

Department of Electrical and Electronics Engineering, Kagoshima University, Kagoshima 890-0065, Japan
Fax: 81-99-285-8396, e-mail: usui@elib.eee.kagoshima-u.ac.jp

The bi-layer film electrodes of TiO₂/Li_xMn₂O₄, which have two functions of opto-electric conversion and electrochemical-energy storage, were prepared by pulsed laser deposition. The Li ratio x in Li_xMn₂O₄ films was changed by changing the oxygen pressure during the deposition to investigate the influence of x on the rechargeability and the photo-rechargeability of the film electrodes. When x increased from $x \sim 1$, the activation energy necessary for the storage of Li ions decreased, and both of the charge/discharge capacity and the photo-charged quantity showed a rapid increase. The excess insertion of Li atoms to Mn sites is considered to increase the number of the storage sites which are effective for the photo-charge by the low photo-emf generated by TiO₂.

Key words: Photo-rechargeable battery, Pulsed laser deposition, Lithium manganese oxide

1. INTRODUCTION

Photo-rechargeable battery is a new device in which two functions of opto-electric conversion and electrochemical-energy storage can be realized in a single electrode[1,2]. In our previous studies[3-5], the problem of chemical instability caused by the photo-induced carriers[6] has been solved by attributing each of the two functions to different materials which are chemically stable. We chose TiO₂ for the opto-electric conversion, and carbon fibers or graphitic carbon films for the storage material[3,4]. However, the photo-charged quantity of the electrodes was much less than that of conventional secondary batteries. The main reason is the small driving force to intercalate Li ions in the electrolyte into the storage material, because obtained photo-emf of ~ 0.2 V with TiO₂ was much lower than the charge voltage of ~ 3 V of Li-ion secondary batteries. Since the magnitude of the photo-emf is limited by the energy gap of TiO₂, it is necessary to increase the storage sites with low activation energy.

It is known that LiMn₂O₄ can realize reversible insertion and desorption of Li ions through three-dimensional network of Li atoms in the spinel structure[7]. The crystal structure of Li_xMn₂O₄ was found to be maintained in a wide range of Li ratio x [8,9], and the diffusion coefficient of Li ions increased with x [7]. Therefore, the distribution of the activation energy necessary for the storage of Li ions is also expected to change with x . With a pulsed laser deposition (PLD) method, the ratio x can be changed widely by the atmospheric pressure of oxygen gas during the deposition[7,9,10].

In this study, the bi-layer film electrodes of TiO₂/Li_xMn₂O₄ with different x were prepared by changing the oxygen pressure with PLD method, and the influence of x on their rechargeability and photo-rechargeability was investigated.

2. EXPERIMENTAL

2.1. Preparation of film electrodes

To ensure the electric conduction, quartz substrates of $50 \times 5 \times 1$ mm³ were covered with Pt film of 230 nm thick by a dc sputtering. After depositing the layer of Li_xMn₂O₄ by PLD on the Pt layer, the layer of TiO₂ was deposited on the Li_xMn₂O₄ layer by the same method. The target of LiMn₂O₄ was prepared by a sintering method. Mixed powder of LiNO₃ and MnO₂ in a stoichiometric ratio was heated at 450 °C for 24 hours in air. The sintered powder was pressed into a disk of 30 mm ϕ \times 5 mm and sintered at 750 °C for 48 hours in air. The target of TiO₂ was also prepared by pressing anatase TiO₂ powder into a disk and by sintering at 450 °C for 6 hours in air.

In PLD method the second harmonics of a Nd:YAG pulse laser (Spectra-Physics Co., GCR-130-10) was used with the pulse width of 7 ns and the repetition rate of 10 Hz. The layer of Li_xMn₂O₄ was prepared with a laser fluence of 3.72 J/pulse \cdot cm² and the substrate temperature of 600 °C. The layers obtained above 5 Torr was too thin to get almost the same thickness for all the Li_xMn₂O₄ layers prepared in different gas pressures. The thickness of ~ 2 μ m was obtained for all the layers below 3 Torr by changing the deposition time from 60 min below 1 Torr to 120 min in 3 Torr. The TiO₂ layer of 400 nm thick was prepared in vacuum with a fluence of 0.85 J/pulse \cdot cm² at a room temperature for 12 min.

2.2. Electrochemical measurements

(a) Constant current charge/discharge measurements

To find the activation energy necessary for the storage of Li ions, the constant current charge/discharge measurements[5] were carried out for film electrodes only with a layer of Li_xMn₂O₄ on Pt layer. The three-electrode cell used in the measurements is shown in Fig.1. A working electrode (WE), a counter electrode (CE) and a reference electrode (RE) were the film

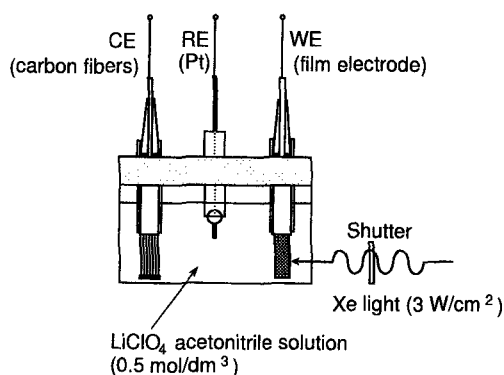


Fig. 1. Experimental cell for electrochemical measurements.

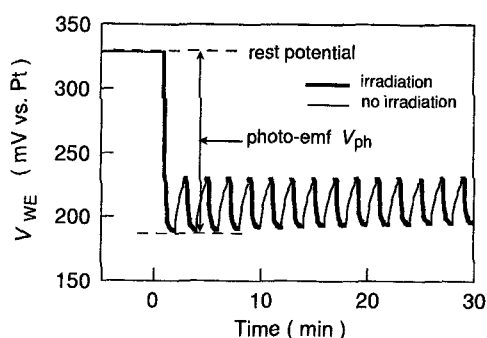


Fig. 2. Variation of V_{WE} obtained for a film electrode of $\text{TiO}_2/\text{Li}_x\text{Mn}_2\text{O}_4$ prepared in 10^{-4} Torr.

electrode, a bundle of carbon fibers and a Pt wire, respectively. The electrolyte was the acetonitrile solution of LiClO_4 (0.5 mol/dm^3). By flowing a constant current of $20 \mu\text{A/cm}^2$ between WE and CE using a galvanostat, a forced charge process and a succeeding forced discharge process were kept without irradiation. The time variation of the potential V_{WE} between WE and RE was measured by repeating these processes of charge and discharge. Because of the irreversible reaction at the interface between the electrode and electrolyte, the charge/discharge curves were unstable at initial several cycles. Therefore, the charge/discharge curves of the fifth cycle were used to compare the charge energy E_{ch} and the charge/discharge capacity Q_{ch} of $\text{Li}_x\text{Mn}_2\text{O}_4$ film electrodes with different Li ratio x .

(b) Photo-emf measurements

To investigate the photo activity of the $\text{TiO}_2/\text{Li}_x\text{Mn}_2\text{O}_4$ bi-layer film electrodes, the photo-emf was measured under the irradiation using the same cell shown in Fig. 1. By opening and closing the shutter, WE of the film electrode was irradiated by a Xe light of 3 W/cm^2 intermittently at an interval of 1 min, and V_{WE} was measured by a potentiostat. Figure 2 shows a variation of V_{WE} obtained for a $\text{TiO}_2/\text{Li}_x\text{Mn}_2\text{O}_4$ film electrode using $\text{Li}_x\text{Mn}_2\text{O}_4$ prepared in 10^{-4} Torr. An alternate drop and rise of V_{WE} was accompanied with the intermittent irradiation. In this study, the potential drop from the rest potential during the irradiation of initial 1 min was defined as the photo-emf V_{ph} .

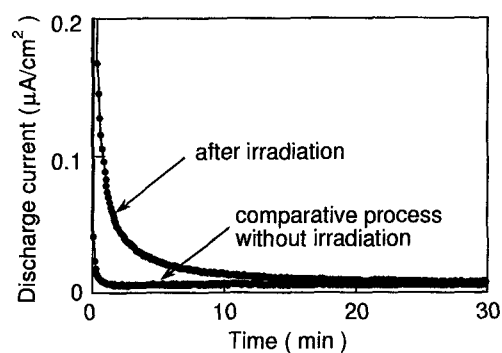


Fig. 3. Discharge currents obtained for a film electrode of $\text{TiO}_2/\text{Li}_x\text{Mn}_2\text{O}_4$ prepared in 10^{-4} Torr.

(c) Photo-rechargeability measurements

To get the photo-charged quantity Q_{ph} , the photo-rechargeability was measured for $\text{TiO}_2/\text{Li}_x\text{Mn}_2\text{O}_4$ film electrodes by using the same cell shown in Fig. 1. First, the shutter was opened, and WE was irradiated for 15 min to photo-charge without connecting WE and CE. After leaving it in the dark for 1 min, the discharge current was measured in the dark for 30 min by connecting WE and CE with a load of $1 \text{ k}\Omega$. Next, the same measurements were made without irradiation for comparison in the dark. Figure 3 shows an example of the discharge currents obtained for a $\text{TiO}_2/\text{Li}_x\text{Mn}_2\text{O}_4$ film electrode using $\text{Li}_x\text{Mn}_2\text{O}_4$ prepared in 10^{-4} Torr. The photo-charged quantity Q_{ph} was defined by the area between two curves of the discharge current with and without irradiation.

3. RESULTS

3.1. Crystal structure

Figure 4 shows XRD patterns of $\text{Li}_x\text{Mn}_2\text{O}_4$ layers prepared in different oxygen pressures. The spinel structure of $\text{Li}_x\text{Mn}_2\text{O}_4$ appeared above 0.01 Torr, while MnO and Mn_3O_4 phases appeared below 0.01 Torr. As shown in Fig. 5, the cubic lattice parameter a of $\text{Li}_x\text{Mn}_2\text{O}_4$ decreased with the oxygen pressure. The Li ratio x in $\text{Li}_x\text{Mn}_2\text{O}_4$ was estimated by using a linear relation of $x = (8.424 - a)/0.191$ obtained from the experimental plots by Xia *et al.* [11]. The increase of x with the oxygen pressure is consistent with the disappearance of MnO and Mn_3O_4 phases in high oxygen pressures. This decrease of a has been attributed to the lattice shrinkage due an increase of Mn^{4+} ratio with smaller ionic radius in $\text{Mn}^{3+}-\text{Mn}^{4+}$ sublattice, rather than the increase of bigger Li^+ ions in the lattice[12]. At above 0.5 Torr, however, x was estimated to be larger than unity similarly to the results obtained for $\text{Li}_x\text{Mn}_2\text{O}_4$ films prepared with PLD method by Morcrette *et al.*[9,10]. The excess Li atoms have been considered to exchange with the Mn atoms in the crystal lattice[8,9].

3.2. Charge/discharge properties at constant currents

Figure 6 shows the charge/discharge curves of $\text{Li}_x\text{Mn}_2\text{O}_4$ film electrodes when the charge process and succeeding discharge process were kept for 30 min. Above 0.1 Torr, potential plateaus appeared both in the charge and discharge processes, showing an occurrence of successive insertion and desorption

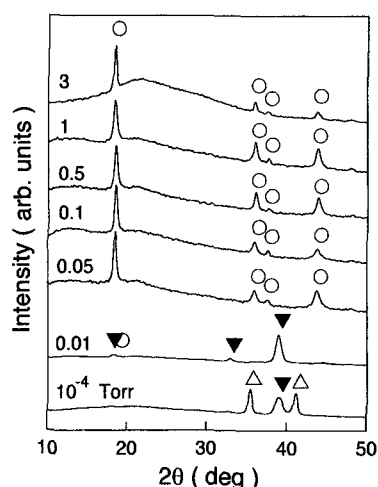


Fig. 4. XRD patterns of $\text{Li}_x\text{Mn}_2\text{O}_4$ films prepared in different oxygen pressures. \circ : $\text{Li}_x\text{Mn}_2\text{O}_4$, \blacktriangledown : Mn_3O_4 , \triangle : MnO .

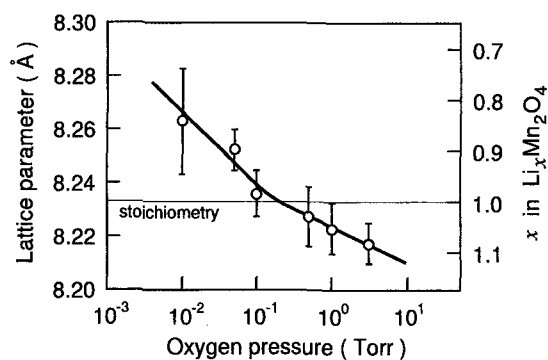


Fig. 5. Oxygen pressure dependence of lattice parameter a and Li ratio x of $\text{Li}_x\text{Mn}_2\text{O}_4$ films.

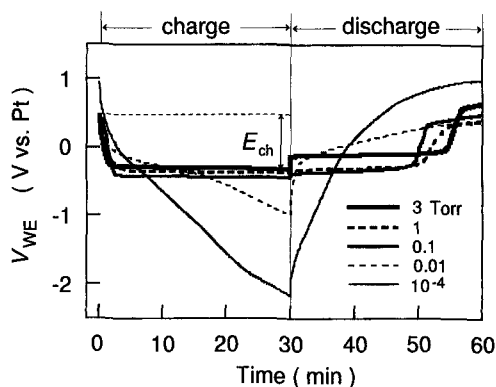


Fig. 6. Charge/discharge curves of $\text{Li}_x\text{Mn}_2\text{O}_4$ film electrodes prepared in different oxygen pressures.

of Li ions. To estimate the energy necessary for the storage of Li ions into the $\text{Li}_x\text{Mn}_2\text{O}_4$ layer, the charge energy E_{ch} was determined from the potential drop in the charge process for 30 min. The charge energy E_{ch} decreased with x as shown in Fig. 7. The charge quantity in the charge process for 30 min corresponds to 8% of the theoretical capacity estimated for $\text{Li}_x\text{Mn}_2\text{O}_4$ when x is assumed to change from 0 to 1.

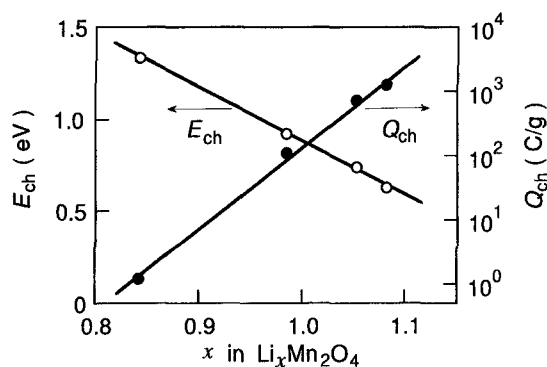


Fig. 7. Charge energy E_{ch} and charge/discharge capacity Q_{ch} as a function of Li ratio x .

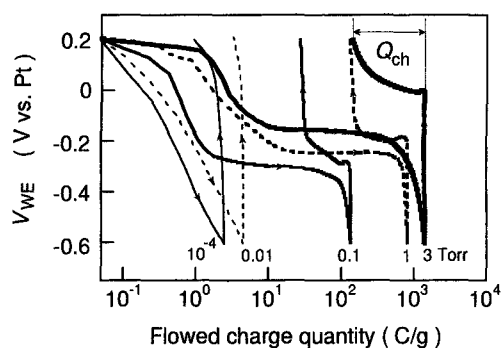


Fig. 8. Charge/discharge curves of $\text{Li}_x\text{Mn}_2\text{O}_4$ film electrodes prepared in different oxygen pressures with cut-off potentials of -0.6 and $+0.2$ V vs. Pt.

To obtain a charge/discharge capacity Q_{ch} with low activation energy, the charge and discharge processes were repeated within the potential range from -0.6 to $+0.2$ V vs. Pt without setting the time limit for each process. As shown in Fig. 8, potential plateaus were observed above 0.1 Torr similarly to Fig. 6. Since an irreversibility remained between the charge and discharge processes even at the fifth cycle, only the discharge capacity shown in the figure was used for the estimation of the charge/discharge capacity Q_{ch} . As shown in Fig. 7, Q_{ch} increased exponentially with x .

3.3. Photo-rechargeability

Figure 9 shows the Li ratio x dependence of the photo-emf V_{ph} and the photo-charged quantity Q_{ph} of $\text{TiO}_2/\text{Li}_x\text{Mn}_2\text{O}_4$ bi-layer film electrodes. No obvious influence of x was found on V_{ph} . This suggests that neither the crystal structure nor the Li ratio x of $\text{Li}_x\text{Mn}_2\text{O}_4$ affect the photo activity of TiO_2 on $\text{Li}_x\text{Mn}_2\text{O}_4$. In contrast, Q_{ph} increased rapidly with x in spite of almost constant driving force of photo-charge generated by V_{ph} . In this study, the maximum Q_{ph} was found for $x = 1.09$ in 3 Torr. This value was about 30 times larger than that obtained for a film electrode prepared in 10^{-4} Torr in which no $\text{Li}_x\text{Mn}_2\text{O}_4$ phase was observed.

4. DISCUSSION

As shown in Figs. 6 and 8, the potential plateaus, which indicate the successive insert and desert of Li

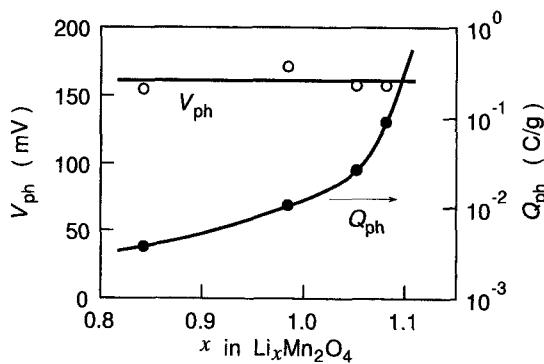


Fig. 9. Photo-emf V_{ph} and photo-charged quantity Q_{ph} as a function of Li ratio x .

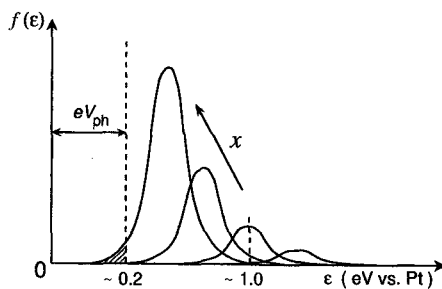


Fig. 10. Distribution of the activation energy $f(\epsilon)$.

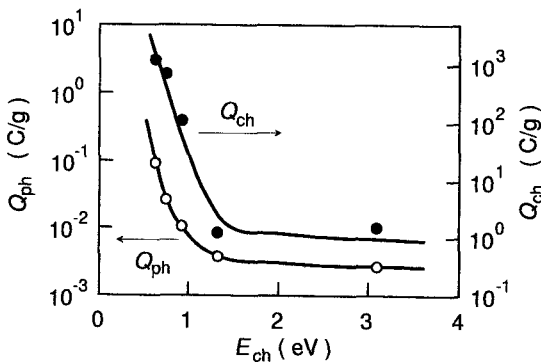


Fig. 11. Relation of the photo-charged quantity Q_{ph} and the charge/discharge capacity Q_{ch} with the charge energy E_{ch} .

ions, appeared above 0.1 Torr, *i.e.* in the region of $x \gtrsim 1$. This shows an existence of very narrow distribution of the activation energy ϵ necessary for the storage of Li ions at 0.7–1.0 eV. Since the charge energy E_{ch} decreased and the charge/discharge capacity Q_{ch} increased with x as shown in Fig. 7, the low energy peak near 1 eV in $f(\epsilon)$ is considered to shift to lower energies, growing rapidly with x as shown in Fig. 10.

In the overdoping region of Li atoms, $x \gtrsim 1$, Mn sites in $\text{Li}_x\text{Mn}_2\text{O}_4$ are known to be occupied by the excess Li atoms [8,9]. Then, the repulsive Coulomb force which acts on the Li ions moving along the network of Li sites will be reduced by the exchange from Mn to Li atoms. Such diffusion path with low activation energy is considered to increase with x .

The maximum Q_{ph} of the electrodes prepared in

this study was only 0.02 % of the theoretical capacity of LiMn_2O_4 . This shows that the energy generated by the photo-emf of TiO_2 was still smaller than the effective activation energy for the charge. Figure 11 shows the relation of the charge/discharge capacity Q_{ch} and the photo-charged quantity Q_{ph} with E_{ch} . Both of Q_{ch} and Q_{ph} showed a rapid increase in the low energy region below 1 eV with the decrease of E_{ch} . Therefore, further increase of Q_{ph} is expected by an increase of the storage sites with low activation energy comparable to the photo-emf as well as the increase of the photo-emf of TiO_2 . Since further increase of the overdoping of Li atoms in $\text{Li}_x\text{Mn}_2\text{O}_4$ might cause a destruction of the spinel structure, it is necessary to find a new dopant to create storage sites with lower energy.

5. SUMMARY

The bi-layer $\text{TiO}_2/\text{Li}_x\text{Mn}_2\text{O}_4$ film electrodes with different Li ratio x were prepared by changing the oxygen pressure with PLD method, and the influence of x on their rechargeability and photo-rechargeability was investigated. The charge/discharge capacity Q_{ch} and the photo-charged quantity Q_{ph} showed a rapid increase with x in particular in the region of $x \gtrsim 1$ at which the Mn sites are occupied by overdoped Li atoms. The rapid increase is attributed to the decrease of the charge energy E_{ch} accompanied with the reduction of the repulsive Coulomb force which acts on the Li ions moving along the network of Li sites. Therefore, order-of-magnitude increases of Q_{ph} are expected by further decrease of E_{ch} down to the same level with the photo-emf of TiO_2 .

REFERENCES

- [1] H. Tributsch, *Appl. Phys.*, **23**, 61-71(1980).
- [2] H. Tributsch, *Solid State Ionics*, **9&10**, 41-58(1983).
- [3] T. Nomiyama, K. Yonemura, X. Zou, Y. Horie and T. Miyazaki, *Trans. Mater. Res. Soc. Jpn.*, **26**, 1251-1254(2001).
- [4] X. Zou, N. Maesako, T. Nomiyama, Y. Horie and T. Miyazaki, *Sol. Energy Mater. & Sol. Cells*, **62**, 133-142(2000).
- [5] H. Usui, O. Miyamoto, T. Nomiyama, Y. Horie and T. Miyazaki, *Sol. Energy Mater. & Sol. Cells*, (2003) in press.
- [6] C. Clement and B. Theys, *J. Electrochem. Soc.*, **131**, 1300-1304(1984).
- [7] C. Julien, E. Poniatowski, M. Lopez, L. Alarcon and J. Jarquin, *Mater. Sci. Engineer.*, **B72**, 36-46(2000).
- [8] Y. Xia and M. Yoshio, *J. Electrochem. Soc.*, **144**, 4186-4194(1997).
- [9] M. Morcrette, P. Barboux, J. Perrière, T. Brousse, A. Traverse and J. P. Boilot, *Solid State Ionics*, **138**, 213-219(2001).
- [10] M. Morcrette, P. Barboux, J. Perrière and T. Brousse, *Solid State Ionics*, **112**, 249-254(1998).
- [11] Y. Xia, H. Takeshige, H. Noguchi and M. Yoshio, *J. Power Sources*, **56**, 61-67(1995).
- [12] J. Marzec, K. Świerczek, J. Przewoźnik, J. Molenda, D. Simon, E. Kelder and J. Schoonman, *Solid State Ionics*, **146**, 225-237(2002).